

**Assessment of nanostructure of “Super Dentin” formation
by application of all-in-one adhesive systems**

Toru Nikaido, Dinesh D. S. Weerasinghe, Go Inoue and Junji Tagami

Cariology and Operative Dentistry, Department of Restorative Sciences

Graduate School, Tokyo Medical and Dental University

Tokyo 113-8549, Japan

Introduction

All-in-one adhesive systems have been widely accepted as simplified bonding procedures in clinic. It was reported that an acid-base resistant zone (ABRZ) was created under a hybrid layer in a self-etching adhesive system at the adhesive/dentin interface, which could contribute against secondary caries formation [1]. However, characteristics of the ABRZ were still unclear. The purpose of this study was to assess nanostructure of the ABRZ by application of all-in-one adhesive systems.

Materials and Methods

Dentin of human premolar was treated with one of two all-in-one adhesive systems; Clearfil Tri-S Bond (TB, Kuraray Medical) and G-Bond (GB, GC) according to the manufacturers' instructions. After placement of a resin composite, the bonded interface was vertically sectioned and subjected to an acid-base challenge in the same manners of the previous study [1]. Following this, the nanostructure of the ABRZ was observed by SEM (JSM-5310LV, Jeol) and TEM (Hitachi H-600, Hitachi).

Results

The SEM observations of the adhesive-dentin interface after the acid-base challenge indicated that the hybrid layer was less than 1 μm thick, and the ABRZ beneath the hybrid layer was observed for each adhesive system. The TEM observations indicated that an electron dense zone (coincident with the ABRZ in the SEM) contained apatite crystallites, of which arrangement and thickness were different between TB and GB.

Conclusions

Application of the all-in-one adhesive systems created the ABRZ at the underlying dentin, which reinforced normal dentin against dental caries. Therefore, this zone may be named “Super Dentin”. Formation of “Super Dentin” will become a key approach in caries prevention in the future.

References

[1] Inoue G, et al. Morphological and mechanical characterization of the acid-base resistant zone at the adhesive-dentin interface of intact and caries-affected dentin. *Oper Dent* 2006; 31: 466-472.

Improved bond performance of dental adhesive system using nano-technology.

Futami Nagano¹, Denis Selimovic², and Hidehiko Sano¹

¹Department of Restorative Dentistry, Graduate School of Dental Medicine, Hokkaido University.
Kita-13, Nishi-7, Kita-ku, Sapporo, 060-8586, JAPAN

²Dental Faculty of Louis Pasteur University, 1,Place de l'Hopital, 67000 Strasbourg, INSERM Institute,
U595, Strasbourg, FRANCE

Since the introduction of the adhesive into dental field, metal-based restoration has been replaced by metal-free restoration. Using the adhesive technology, minimum invasive technique has been possible in daily clinical practice as well as esthetic tooth-colored restorations have become very popular among Japanese dentists.

In the last decade, two approaches to dentin bonding were introduced in the field of adhesive dentistry, “moist bonding system” and “self-etching priming system.” In 90’s, the moist bonding was dominant in the world market compared to the self-etch approach. However, when using the moist approach, postoperative sensitivity and technique sensitivity were getting to be a big issue for clinical use. Moreover, current in vivo and in vitro works revealed that the moist bonding to dentin degraded within several years. Based on the current findings of the moist approach, the trend of the use of adhesives seems to be shifting to the self-etch approach.

Self-etching primers were designed to infiltrate resin monomers into superficial tooth surface simultaneously with the self-etching process, by which the risk of existence of demineralized dentin at the adhesive interface is very low or nothing. Theoretically, the self-etch approach is less technique sensitive and lower rate of inducing the post-operative sensitivity. Moreover, the self-etch approach should create more durable bonds between resin and dentin compared to the moist approach because of the lack of the demineralized dentin at the adhesive interface.

Current issue of the dental adhesive would be technique sensitivity and durability of bond between tooth structure and adhesive resin. Several approaches have been done to overcome the issue. Self-etching approach is believed to create durable bond because demineralization of superficial tooth surface is very shallow. Other approach is to use the inhibitor of enzymes that are always secreted within the oral environment. [1]

Recently, we have found the third possibility to increase the durable bond. We used platinum nano-colloid solution as a pretreatment agent. [2] Adhesive resin used was 4-META/MMA-TBB. Conditioning agent was 10% citric acid solution containing 3% ferric chloride. When using the solution, we observed doubled bond strength. This implies that the use of platinum nano-colloid solution would create higher conversion at the interface than conventional bonding procedure. Proper use of nano-colloid can increase the bond strength and create durable bond in the clinical situation.

Further studies are necessary to find out useful way of application of the nano-colloid for clinical use.

References

- [1] H. Sano: J Dent Res 85(1): 11-14, 2006 [2] M. Kajita et al. Free Radic Res June; 41(6): 615-26, 2007

Novel Preparation Method of Environmental Catalysts and their Application

Atsushi Muramatsu¹

¹Institute of Multidisciplinary Research for Advanced Materials, Tohoku University

Katahira 2-1-1, Aoba-ku, Sendai 980-8577, Japan

Introduction. Environmental catalysts, so-called green catalysts, are roughly divided into 2 groups, that is, production and removal catalysts. The typical one of the former is the photocatalyst to give hydrogen as a clean energy, and the latter the reduction and/or conversion catalysts of wastes poisonous for earth and/or life. In this presentation, titania, which has been recognized as an excellent catalyst for hydrogen production from water since the discovery of Honda and Fujishima [1], will be focused, but it absorbs only ultraviolet light in sun shine because of the wide band gap, 3.2 eV, for anatase. The attempt to shift it visible light region has been tried mainly by the incorporation of hetero-metal into Ti-O bond in place of O [2]. In this presentation, I will introduce our trial to shift the band gap by the partial sulfurization to TiO₂ nanoparticles prepared by Gel-Sol method, and to make photocatalyst thin film generated by ACPLD, the Atmosphere-Controlled Pulsed Laser Deposition, followed by selective deposition of Ni-based nanoparticles by CVRD, the Chemical Vapor Reductive Deposition, which both of them has been originally developed by ourselves. In particular, the hydrogen evolution, in the reaction of ethanol to acetaldehyde, was markedly improved for the latter case.

Experimental. Titanium dioxide used in this work was purchased from Wako Pure Chemicals Ind. Ltd. Pelletized and subsequently calcined titanium dioxide target (identified as rutile phase from XRD measurement) was ablated by Nd:YAG pulse laser (LAB170-10, Spectra Physics) under the vacuum of less than 6.7×10^{-5} kPa to form a thin film on a quartz glass substrate [3]. The laser beam employed has 1064 nm of wavelength and 1.01 J cm^{-2} of energy density. The size of the quartz glass substrate is 12 mm-square and 1 mm thickness. For the preparation of sulfur-doped thin film, vaporized carbon disulfide was introduced into the ablation chamber to control the inner pressure at 2.1×10^{-2} kPa. Nickel nanoparticles were deposited on the sulfur-doped titanium dioxide thin film by the chemical vapor reductive deposition method [4]. Prior to the deposition, a horizontal tube made of Pyrex glass was purged twice by nitrogen gas and then evacuated to less than 1.0×10^{-2} kPa. Nickelocene (Wako Pure Chemicals) as nickel precursor and hydrazine monohydrate (Wako Pure Chemicals) as reducing agent were introduced into the glass tube and allowed to react on the surface of thin film substrate kept at 100 °C. The procedure did not greatly affect the properties of neither the sulfur-doped nor undoped titanium dioxide thin film. After 10 minutes of reaction the residual vapor was evacuated, and nitrogen gas was filled before cooling the film to room temperature.

Results and Discussion. Sulfur-doped titanium dioxide thin film was successfully prepared by atmosphere-controlled pulsed laser deposition. UV-vis and XPS studies demonstrated that sulfur atoms were substituted for oxygen atoms of titanium dioxide lattice to induce visible light sensitivity. Doping of sulfur showed a negative effect on crystallization of titanium dioxide thin film, and resulting material was amorphous as evidenced by SAED measurement. However, the photocatalytic activity was enhanced by sulfur doping. In addition, nickel nanoparticles deposited on the surface of thin film by chemical vapor reductive deposition method remarkably increased the photocatalytic activity in hydrogen evolution or dye decoloration.

References

- [1] A. Fujishima, K. Honda, *Nature* **1972**, 238, 37.
- [2] R. Asahi, T. Morikawa, T. Ohwaki, K. Aoki, Y. Taga, *Science* **2001**, 293, 269. J. Cuya, N. Sato, K. Yamamoto, A. Muramatsu, K. Aoki, Y. Taga, *Thermochimica Acta* **2004**, 410, 27.
- [3] T. Nakamura, T. Ichitsubo, E. Matsubara, A. Muramatsu, N. Sato, H. Takahashi, *Scripta Mater.* **2005**, 53, 1019.
- [4] M. Yoshinaga, H. Takahashi, K. Yamamoto, N. Sato, A. Muramatsu and T. Morikawa, *J. Colloid and Interface Sci.* **2007**, 309, 149.

Comparative Studies of Carbon Nanofiber Cytotoxicity on Young and Senescent cells of *Paramecium*

¹Nobuyuki Haga, ¹Taiki Abe and ¹Koichi Haneda

¹Ishinomaki Senshu University, Ishinomaki, Miyagi 986-8580 Japan

Paramecium is a eukaryotic unicellular organism with a well-defined life history. The beginning event of life history is conjugation between two cells of complementary mating types. Like human being, *Paramecia* show sexual immaturity, maturity and senescence according to the accumulation of the total number of cell divisions after conjugation. Therefore the age of *Paramecia* is calculated by the number of total cell divisions instead of physical time. The immaturity period is about 50 and the life span is about 1,000 cell divisions under our experimental conditions.

Carbon nanofibers (CNF) is expected to be very useful in wide variety of technology including biomedicine and human health. Although our previous studies demonstrated that CNF does not have serious cytotoxicity on young *Paramecia*, little is known about the cells undergoing senescence. In this study we compared CNF cytotoxicity by using two different ages of *Paramecia*, 50 (young) and 750 (senescence or old) cell divisions after conjugation. Cell proliferation activities of both young and old *Paramecia* were slightly decreased in fresh culture medium under the presence of 50 μ g/ml of CNF to compare with untreated controls. The dose effect curves of CNF showed no significant difference between young and old *Paramecia*. However, there was clear difference in the proliferative activity after removal of CNF from the culture medium suggesting that the reversibility of old *Paramecia* are lower than that of young one. In addition, the dose effect curves of post-mitotic cell survival in phosphate buffered saline under the presence of 50 μ g/ml of CNF showed that the viability of old *Paramecia* is reduced to about 50% of young cells.

Our results indicate that the cells of senescent *Paramecia* are more sensitive to CNF than young cells, although, in both ages, the cytotoxicity of CNF is not lethal. The mechanism of CNF effect on *Paramecium* proliferation and survival will be discussed.

Studies of *Paramecium caudatum* by Means of Scanning Electron
Microscope and Projection X-Ray Microscope

¹Keiji Yada, ²Taiki Abe and ²Nobuyuki Haga

¹Tohken CO., LTD, 2-27-7 Tamagawa Chofu, Tokyo 182-0025 Japan

²Ishinomaki Senshu University, Ishinomaki, Miyagi 986-8580 Japan

Paramecium is a very interesting unicellular organism for study of cell physiology and therefore seems interesting for nanotoxicology assessment. Samples of *Paramecia caudatum* cultivated by the lettuce juice method are observed with a scanning electron microscope (SEM) and a projection X-Ray microscope (XRM) containing computer tomography (CT) function. Samples prepared by natural drying are not suitable to observe fine structures because of flattening effect in the drying process so that two kinds of fixatives, glutaraldehyde and osmium-tetra oxide acid, are employed. After the fixation and replacement procedures with suitable alcohol, the samples followed by a critical point drying or a freeze drying, well retain their structures. Surface structures of *P. caudatum*, cilia and microfibrillar systems including infraciliary lattice structures, are clearly depicted by SEM observation.

On the other hand, however, XRM images give quite different information, namely, the structures of internal organelles like the macronucleus placed in the central part of cell body and a large number of trichocyst tips located under the cell membrane of a whole body are visible. In the case of glutaraldehyde fixation, the surface structures and internal structures are both visible though their image contrast is fairly weak.

CT images of *P. caudatum* treated by osmium-tetra oxide acid fixation followed by freeze drying are taken under the imaging condition of 20 kV accelerating voltage with W-target. Image contrast of an individual projection X-ray image taken by the above mentioned condition is very weak but that of the CT image is remarkably enhanced. Any cross section of desired position and direction can be displayed by CT so that it is very helpful to grip a relative arrangement of internal organelles especially when compared with the corresponding X-Ray projection image .

P. caudatum samples treated in the environmental condition containing nano-particles of Ag (17 nm across) and Co ferrite (300 nm across) are also observed by the same ways whose results will be reported.

Designer Functionalized Self-assembling Peptide Nanofiber Scaffolds for the Growth, Migration, and Tubulogenesis of Human Umbilical Vein Endothelial Cells

Xiumei Wang¹, Shuguang Zhang²

¹Biomaterials Laboratory, Department of Materials Science and Engineering, Tsinghua University, Beijing 100084, China

²Center for Biomedical Engineering, Massachusetts Institute of Technology, Cambridge, MA 02139, USA

A class of designer self-assembling peptide nanofiber scaffolds as a unique biological material has diverse and broad applications including for 3-D tissue cell culture, slow drug release, regenerative medicine, and tissue engineering [1,2]. One of these peptide scaffolds, RADA16-I (AcN-RADARADARADARADA-CONH₂) has been used in bone, cartilage, and neural regeneration studies that have shown great promises [3]. We develop several new functionalized self-assembling peptide nanofiber scaffolds designed specifically for angiogenesis study through directly coupling pure RADA16-I with short biologically angiogenic motifs [4]. Angiogenesis is very important in regenerative medicine. An adequate blood vessel supply to the newly formed tissue and within the transplanted scaffold is essential in determining the success of new tissue regeneration [5]. In our study, two designer functionalized peptides, KLT (VEGF mimicking peptide) and PRG (2-unit RGD repetitive peptide) significantly enhanced endothelial cell survival, proliferation, migration, and morphological tubulogenesis compared with pure RADA16-I scaffold. The designer functionalized peptide solutions were mixed in a volume ratio of 1:1 with 1% (W/V) pure RADA16-I solution to get 1% functionalized peptide mixtures (RAD/PRG or RAD/KLT), which underwent self-assembly and incorporation to form uniform and interweaved long nanofibers (Fig. 1). The proliferation result showed that the cell numbers on RAD/PRG and RAD/KLT were about 1.5 times as many as that on RADA16-I after one-day culture, which suggested that the cells behavior was positively affected by the functional motifs of PRG and KLT. This proliferation result was also consistent with the morphologic observations from fluorescence microscopy examinations. Besides cell survival and proliferation, the functional motifs PRG and KLT also induced endothelial cells migrated from RADA16-I to/on these functionalized peptide mixtures scaffolds. In most *in vitro* angiogenesis models, endothelial cells undergo morphological differentiation and reorganized into an extensive network of capillary like structure in both short-term and long-term cultures depending on matrix and culture conditions. In our current studies, HUVECs seeded on 2-D designer RAD/KLT scaffold rearranged into capillary-like structure network as early as 4 hr after seeding and remained intact for up to 3 days. Furthermore, it is observed that endothelial cells in 3-D environment were elongated with many cellular

protrusions rather than the characteristic cobblestone and flattened morphology. In 3-D environment, both pure RADA16-I and functionalized peptide scaffolds could facilitate endothelial cells to undergo tubulogenesis and form capillary-like structure through cellular reorganization of one cell (Fig. 2, image a and b) or cellular connection of two or more cells (Fig. 2, image c). In brief, our results suggest that the designer functionalized peptide scaffolds have a great promise for promoting endothelial cell growth, migration, and tubulogenesis, which might be very useful for diverse tissue engineering and regeneration.

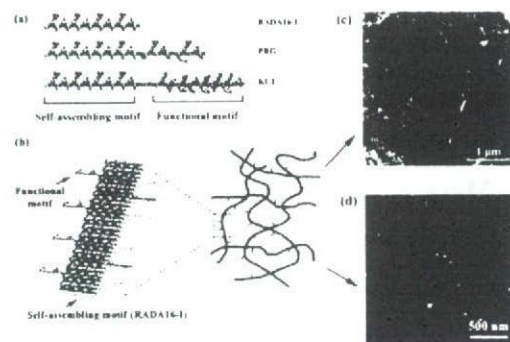


Fig. 1 Molecular models of designer peptides and schematic illustrations of self-assembling peptide nanofiber scaffolds.

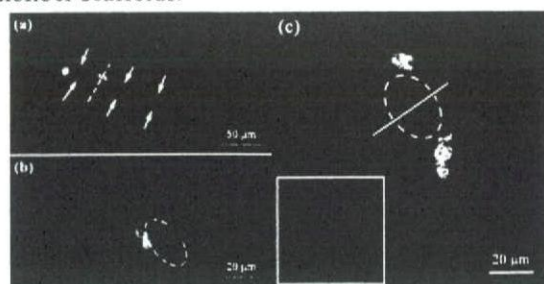


Fig. 7 Tubulogenesis in 3D cell culture.

References

- [1] S. Zhang, Nat. Biotechnol. Vol. 21 (2003), p. 1171
- [2] S. Zhang, T. C. Holmes, C. Lockshin, et al., Proc. Natl. Acad. Sci. USA Vol. 90 (1993), p. 3334
- [3] Horii, X. M. Wang, F. Gelain, et al., PLoS One Vol. 2 (2007), p. e190
- [4] L. D. D'Andrea, G. Laccarino, R. Fattorusso, et al., Proc. Natl. Acad. Sci. USA Vol. 102 (2005), p. 14215
- [5] D. J. Mooney and A. G. Mikos, Sci. Am. Vol. 280 (1999), p. 60

Modification of porphyrin precursor 5-ALA with TiO₂ particles by ultrasound irradiation in vitro and treatment of the administrated cancer model by ultrasound in vivo.

Norio Miyoshi*, Yukihiro Fukunaga*, Toshiyuki Ogasawara**, Hidetaka Kinoshita**, Tsuyoshi Miyasaka***, and Haruo Hisazum****

Division of Tumor Pathology, Department of Pathological Sciences, **Department of Dentistry and Oral Surgery, Faculty of Medicine, University of Fukui, Matsuoka #23-3, Eihei-ji-cho, Yoshida-gun, Fukui 910-1193, *Faculty of Biomedical Engineering, Toin University of Yokohama, Tetsu-mati #1614, Aoba-ku, Yokohama 225-8502, ****Tera-machi #3-1-20, Kanazawa 921-8033, Japan.*

[Aim]: To carry the nano-particles of TiO₂ into cancer tissue a precursor (5-aminolevulinic acid) of protoporphyrin (Pp-IX) was modified with the particles before the administration into the experimental tumor model mouse.

[Materials and Methods]: (1) Modification of TiO₂ particles: TiO₂ particle sol aqueous solution was mixed and modified with 5-ALA solution by an ultrasound irradiation. The particles has an affinity with 5-ALA after treating by the ultrasound irradiation. The particles with 5-ALA were fractioned at the border in the BuOH:Acetic Acide: H₂O (= 4:1:5) mixed solution. Furthermore, the modified particle solution was oral administrated into the transplanted tumor (squamous cell carcinoma) C3H/He mouse. The distribution of the TiO₂ particles in the tumor tissue were recognized by a Raman spectromicroscope to create the mapping image. (2) Distribution of the TiO₂/Pp-IX particles in the experimental tumor tissue by FT-IR and Raman microscopes. (3) Treatment of the experimental tumor by

irradiation with laser (635 nm) and ultrasound (47 kHz).

[Results]: (1) The distribution of the particles of Pp-IX/TiO₂ was observed in the blood vessel in the tumor tissue as dots sized of 1 μm diameter. It was found that the signal of OH radical adducts with a spin trap reagent of DMPO was enhanced by the ultrasound irradiation comparing that of without the particles in the solution using an electron spin resonance (ESR) instrument. (2) The distribution of the particles in the tumor tissue was presented in the blood vessel of the tumor tissue observed by FT-IR⁽¹⁾ and Raman spectroscopie. (3) The therapeutic effect of cancer was confirmed by the observation of reduced the tumor size after the treatment with laser and ultrasound irradiations.

[References]

[1] N. Miyoshi, H. Kinoshita, and T. Moriwaki: FT-IR image of TiO₂/Pp-IX particles in tumor tissue. *Am. Inst. Phys.*, **902**: 77-78, 2007.

Invited-6

Development of a second-generation radiofrequency ablation using sintered MgFe_2O_4 needles and alternating magnetic field for human cancer therapy

Yuji Watanabe¹, Koichi Sato¹, Shungo Yukumi¹, Motohira Yoshida¹, Yuji Yamamoto¹, Yuji Doi¹, Takashi Naohara², Tsunehiro Maehara³, Hiromichi Aono², Kanji Kawachi¹

¹Department of Organ Renererative Surgery, Ehime University Graduate School of Medicine, Toon-shi 791-0295, Japan, ²Department of Materials Science and Engineering, Faculty of Engineering, Ehime University, Bunkyo-cho 3, Matsuyama 790-8577, Japan, ³Department of Physics, Faculty of Science, Ehime University, 790-8577, Japan

Backgrounds and Methods: Radiofrequency ablation (RFA) utilizing heat generated by an alternating current (AC) of 470kHz is widely performed as minimally invasive local treatment for liver tumors and other solid cancers. However, RFA has some problems resulting from dielectric heating including a necessity to hold an electrode during treatment and difficulty in repeatability. This study investigated the efficacy of a novel thermotherapy for solid cancers utilizing a sintered MgFe_2O_4 needle and AC magnetic field in xenograft rat models mimicking human liver cancer and breast cancer. A thin needle made from MgFe_2O_4 particles was prepared by sintering at 1100 °C and inserted into the tumor transplanted in the liver or subcutaneous tissue mimicking liver cancer or breast cancer, respectively. Tumors were then heated under an AC magnetic field, 4 kA/m, for 10 to 30 min. We monitored the temperature of rat tissue during treatment and sequentially evaluated histological changes and hepatocyte cellular activity after heat stimulus by using nicotinamide adenine dinucleotide (NADH) diaphorase staining and TUNEL staining including other evaluations of apoptosis. **Results:** The mean temperature of the tumor during heating was controlled around 60 °C [1-3]. No viable tumor cells were observed 28 days after treatment histologically. The injury area spread progressively until 3 days after heating, when the area was surrounded by fibroblasts, with hepatocytes or smooth muscle cells positive for TUNEL staining [1-3]. **Conclusion:** This is the first time that a ferrimagnetic ferrite heating device under an AC magnetic field has achieved a temperature beyond 60°C and led tumor to complete cell death. This would be a useful device for a local control of cancers.

Literature References: [1] K.Sato, Y.Watanabe and A.Horiuchi: J.Surg.Res. (in press), [2]K.Sato, Y.Watanbe and A.Horiuchi: J.Gastroenterol.Hepatol. (in press), [3] S.Yukumi, Y.Watanabe and A.Horiuchi: Anticancer Res.Vol.28(2008), p.69

Possibility of Drug Delivery System (DDS) with ability of collagen fiber formation

Kikuji Yamashita¹, Akemichi Ueno², Tatsuo Ishikawa¹, Kaori Sumida¹, Kaori Abe¹ and Seiichiro Kitamura¹

¹Department of Oral and Maxillofacial Anatomy, Institute of Health Bioscience, University of Tokushima Graduate School, Kuramoto, Tokushima 770-8504, Japan

²Department of Hygiene Chemistry, School of Pharmaceutical Sciences, Ohu University, Misumido, Tomita-machi, Koriyama, Fukushima, 963-8611, Japan

Introduction

Collagen was well known to stick close together to various materials containing drugs and to be a member of extra cellular matrix of various connective tissue containing bone, cartilage and adipose tissue. Then, in order to estimate that collagen was suitable supporting materials for Drug Deriver System (DDS) or not, the movement of collagen at the surface of titanium and hydroxyapatite was analyzed.

Materials and Methods

Commercially pure titanium plates (cpTi) (length; 20mm, width; 10mm, thickness; 1 mm) were immersed in α -Minimal Essential Medium (α -MEM: Gibco, Grand Island, NY, USA) at 37°C for 3 weeks for calcification. The surface was analyzed by X-ray microanalysis and X-ray diffraction. The 200 μ l of a 5×10^5 /ml MC3T3-E1 cells obtained from the Riken Cell Bank (Tsukuba, Japan) were cultured on calcified titanium plates in α -MEM with 10 % fetal bovine serum (FBS: Firtoron, Australia), 50 μ g/ml freshly prepared L-ascorbic acid 2-phosphate (Sigma, St. Louis, MO, USA).

On day 1, 3, 5, 7, 10 and 14, four titanium cultures were fixed with 1.5% glutaraldehyde and paraformaldehyde in 0.1 M phosphate buffer (pH 7.4), and stained with 2% uranyl acetate in 50% ethyl alcohol for 2 hours. After post-fixation with 2% osmium in 0.1 M phosphate buffer (pH 7.4), the samples were dehydrated in graded alcohols and critical-point dried in CO₂ (HCP-2: Hitachi, Tokyo, Japan). The titanium plates with cells at the surface were detached with adhesive tape, thinly sputtercoated with gold (about 20nm) (Eiko Engineering, Tokyo, Japan), and examined with a scanning electron microscope (JSM5300, Jeol, Tokyo, Japan) and a field emission scanning electron microscope (JSM-6335F, Jeol, Tokyo, Japan).

Results and Discussion

After 1 week in culture medium, the calcification on the surface of titanium plates without any cell was in the form of rod-like structures about 100 nm wide. Within 3 weeks, these rods had grown and fused with each other to form dome-like structures with a smooth surface. X-ray microanalysis and X-ray diffraction analysis confirmed that the dome-like structures were a form of calcification consisting of apatite lattice.

Each dome-like calcification structure on the titanium plates was covered with smooth-surfaced nodules out of which many growing collagen fibers protruded after 3 days in culture with MC3T3-E1 cells. The one tip of beads-like collagen fiber with spherical granules bound to the calcified bioactive layer of titanium and hydroxyapatite and another tip continued to grow (Fig. 1) [1]. These collagen fibers had joined together to form a network after 7 days in culture [2]. The results suggested that when nano beads of collagen were used as supporting materials of DDS, the collagen beads with drugs remained at the peculiar tissue consisted of same type of collagen as collagen fiber combined to tissue. Therefore, nano beads of collagen were considered to be suitable supporting materials for DDS being able to apply to various connective tissues.

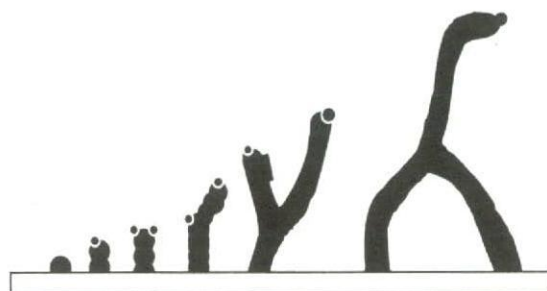


Figure 1. Model of collagen fiber formation

[1] S. Eguchi, K. Yamashita and H. Morimoto, et. al.: Connect. Tissue Vol.36 (2004), p.9

[2] K. Yamashita, S. Eguchi and H. Morimoto, et. al.: Connect. Tissue Vol.36 (2004), p.1

Calcium phosphate nanoparticles for cell transfection

Anna Kovtun, Matthias Epple

¹Inorganic Chemistry, University of Duisburg-Essen, Essen, Germany

Transfection is a widely used method in molecular biology for the introduction of foreign nucleic acids (DNA or RNA) into eukaryotic cells. This permits the control of intracellular processes, e.g. the induction of protein expression or gene silencing. Nucleic acids alone cannot penetrate the cell membrane therefore special carriers like cationic polymers or inorganic nanoparticles are required.^[1] Calcium phosphate nanoparticles as carriers are very promising because of their high biocompatibility and easy preparation.

We prepared single-shell and multi-shell calcium phosphate nanoparticles, and functionalized them with DNA and siRNA. Thereby, the expression of enhanced green fluorescing protein (EGFP) can be induced (by using pcDNA3-EGFP^[2]) or silenced (by using siRNA^[3]). The single-shell nanoparticles were prepared by rapid mixing aqueous solutions of calcium nitrate and diammonium hydrogen phosphate. The multi-shell nanoparticles were produced by adding further layers of calcium phosphate and DNA to protect DNA from the intracellular degradation by endonucleases. The size of the nanoparticles according to dynamic light scattering and electron microscopy was 30-50 nm with a zeta potential around -30 mV. The transfection efficiency of the nanoparticles was tested by cell culture experiments.

The nanoparticle dispersion is stable and can be stored at 4 °C for two weeks without loss of activity, making it available as biochemical reagents for gene therapy.

References

- [1] V. Sokolova and M. Epple: *Angew. Chem. Int. Ed.* Vol. 47 (2008), p. 3182
- [2] V.V. Sokolova, I. Radtke, R. Heumann and M. Epple: *Biomaterials* Vol. 27 (2007), p. 1347
- [3] V. Sokolova, A. Kovtun, O. Prymak, W. Meyer-Zaika, E. A. Kubareva, E. A. Romanova, T. S. Oretskaya, R. Heumann and M. Epple: *J. Mater. Chem.* Vol. 17 (2006), p. 721.

Magnetic Drug Targeting

Urs O. Häfeli

University of British Columbia, Faculty of Pharmaceutical Sciences
2146 East Mall, Vancouver, BC V6T 1Z3, CANADA

Conceptually, magnetic drug delivery by particulate carriers is a very efficient method of delivering a drug to a localized disease site. Very high concentrations of chemotherapeutic or radiological agents can be achieved near the target site, for example in a tumor, without any toxic effects to normal surrounding tissue. In this talk, historic and current biological applications of magnetic microspheres and nanospheres will be discussed. Future directions and problems that still need to be overcome for efficient and beneficial use of magnetic carriers in biological applications and clinical practice will be highlighted.

Magnetic carriers [1] receive their magnetic responsiveness to a magnetic field from incorporated materials (magnetite, iron, nickel, cobalt) and are normally grouped according to size, starting at 4-6 nm in diameter (ferrofluids, nanospheres) up to 1-100 μm (magnetic microspheres) [Fig. 1]. Often, magnetic liposomes are also included when speaking about magnetic carriers.

For biomedical applications, magnetic carriers must be water-based, biocompatible, non-toxic, and non-immunogenic. For the first

medical applications magnetite or iron powder were directly applied. Better biocompatibility, however, was reached by encapsulating the magnetic components with matrix materials such as chitosan, dextran, poly(lactic acid), or albumin.

Magnetic microspheres can be used *in vivo* as contrast agents in magnetic resonance imaging (MRI) [2]; as cancer treating agents for example in radioactive form, loaded with chemotherapeutic drugs, or used directly for magnetic fluid hyperthermia under the influence of an externally applied AC magnetic field [3]; as remotely activated drug reservoirs; or for the separation of cancer cells from healthy cells, thus allowing better and side effect free stem cell transplantation.

For more information about magnetic carriers and an extensive bibliography of this field, please visit the "Magnetic Carrier Home Page" at <http://www.magneticmicrosphere.com>.

Reviews about magnetic particles

- [1] D. Horak, M. Babic, H. Mackova, M.J. Benes. *J. Sep. Sci.* Vol 30 (2007), p. 1751-72.
- [2] L.X. Tiefenauer. In: T. Vo-Dinh: *Nanotechnology in biology and medicine: methods, devices, and applications*, (CRC Press, Taylor and Francis, Boca Raton, FL, 2007), Section D Nanomedicine applications D1. p. 1-20.
- [3] W. Andrä, U.O. Häfeli, R. Hergt, R. Misri. In: H. Kronmüller, S. Parkin: *The Handbook of Magnetism and Advanced Magnetic Materials* (John Wiley & Sons Ltd., Chichester, UK 2007), vol 4., 2536-2568.

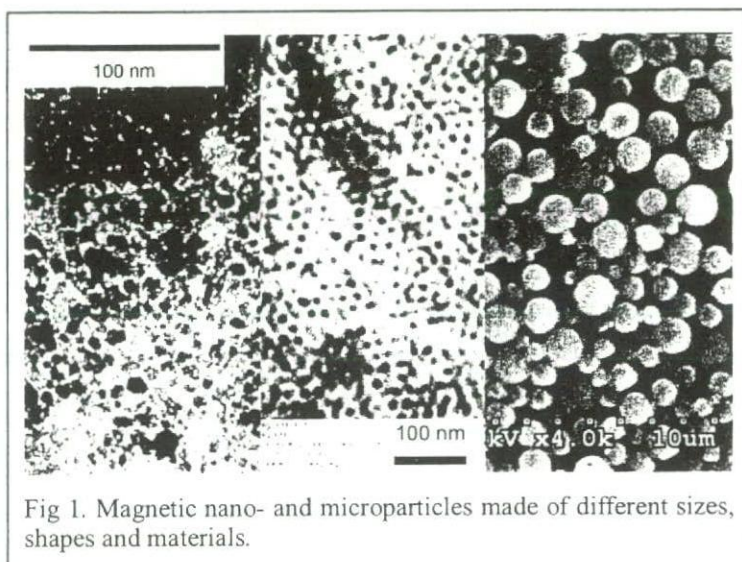


Fig 1. Magnetic nano- and microparticles made of different sizes, shapes and materials.

In-situ observation of Ag nanoparticles at high temperature

Tetsu Yonezawa

Department of Chemistry, School of Science, The University of Tokyo,
Hongo, Bunkyo-ku, Tokyo 113-0033, Japan

Silver nanoparticles have been considered as the most promising materials for preparation of micro (or nano)-wiring or thin electrodes. Until now, various chemical companies tried to prepare suitable silver nanoparticles for low temperature sintering. In this study, we have used an *in-situ* hot sample holder for TEM to reveal the structure changes of silver nanoparticles at high temperature.

Silver nanoparticles were provided from Bando Chemical, Japan. Size distribution of these silver nanoparticles were relatively wide (15 ~ 40 nm). The particles were covered by organic acid for stable dispersion. We put the sample dispersion in carbon-coated tungsten coil. This coil was heated up to 1500 °C by DC current. The images were taken by using a Hitachi HD-2300 or HF-2000 electron microscopy.

When the nanoparticles were heated, small particles show lower contrast and no lattice fringes. This phenomenon strongly indicates that smaller nanoparticles became amorphous at lower temperatures than larger nanoparticles. In fact, very small metal nanoparticles usually show lower melting point. The smaller particles incorporated to the larger ones at higher temperature (Figure 1 right). Therefore, it is very reasonable that mixed dispersion of smaller nanoparticles and larger ones show a lower sintering temperature. Of course, smaller nanoparticles show a lower sintering temperature but they may show a higher resistivity.

This work has been carried out through Collaboration of Regional Entities for the Advanced of Technological Excellence (CREATE) organized by Hyogo Prefecture funded by Japan Science and Technology Agency (JST).

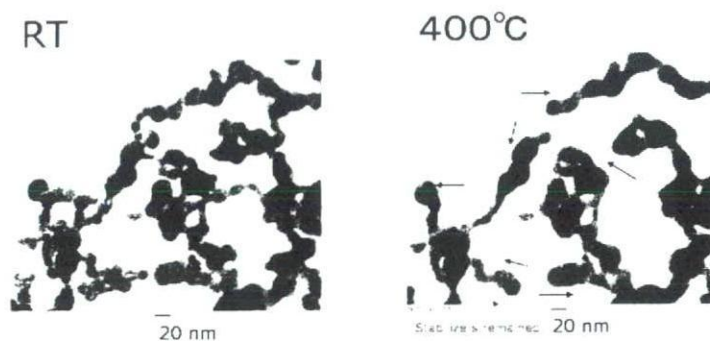


Figure 1. Silver nanoparticles observed on an *in-situ* hot sample holder.

Fabrication and influence of heat treatment on nano-structured titanium oxide

Madhav Prasad Neupane¹, Kim Yu Kyoung¹, Il Song Park², Min Ho Lee^{2*}, Tae Sung Bae², Fumio Watari³

¹Department of Bionanosystem Engineering, Chonbuk National University, Jeonju 561-756, Republic of Korea.

²Department of Dental Biomaterials, School of Dentistry, Chonbuk National University, Jeonju 561-756, Republic of Korea

³Biomedical, Dental Materials and Engineering, Dept. of Oral Health Science, Graduate School of Dental Medicine, Hokkaido University, Sapporo, Japan, 060-8586

OBJECTIVES OF RESEARCH: Nanotubular materials have attracted tremendous attention due to their exceptional electronic and mechanical properties. Since the discovery of carbon nanotubes [1] the extensive research has been carried out to explore nanotubular materials other than carbon, including the oxide materials titania, alumina, zirconia, and silica. Recent interest has focused on the creation of nanotube structures of these ceramics [2, 3], especially that of titania which has a wide range of technologically relevant applications such as gas sensors, photovoltaics, photo and thermal catalysis, photoelectrochromic devices, and immobilization of biomolecules.

This paper investigates the oxidation process of titanium in HF/H₂SO₄ solution via constant-voltage experiments. We have subjected titania nanotube arrays prepared by anodization to high-temperature annealing, up to 600°C in oxygen to understand their temperature stability as well as structural and morphological transformations.

EXPERIMENTAL: The samples were anodized in 1M H₂SO₄/0.16MHF by using a two electrode configuration. The TiO₂ nanotubes were prepared using a 20V for 2 h at room temperature. Characterization was done by FE-SEM and XRD.

RESULTS AND DISCUSSION: From FESEM images it can be seen that the nanotube array is uniform over the substrate annealed at 450°C. The diameter of nanotube calculated from FESEM images was 50-100nm. The nanotube architecture annealed at 500°C was coalesced but the sample still possesses porosity. The sample heated to 600°C shows that the porosity completely disappeared because of grain growth leaving dense rutile crystallites.

XRD patterns shows the as-deposited films were found to be amorphous. The anatase phase was appeared at 450°C and below this temperature. At 500°C complete transformation of anatase to rutile occurred. At 600°C the rutile peak becomes more intense. From XRD it can be seen that the reflections from the titanium support decreased as the annealed temperature increased and crystallinity of rutile titania increased. This shows that the titanium support became oxidized and transformed to crystalline titania at high temperatures. It indicates that the grain size of rutile progressively increased with temperature after its nucleation. In contrast, the size of anatase grains shows a decreasing trend.

CONCLUSIONS: The samples prepared using an anodization voltage of 20 V, consisting of well-defined nanotube arrays were found at 450°C. However, at higher temperatures the crystallization of the titanium support disturbed the nanotube architecture causing it to collapse and densify. When subjected to annealing in oxygen at 500°C, the tubes coalesced completely and formed a wormlike pattern. At 600°C the dense rutile crystals were obtained. The anatase phase was appeared at 450°C through XRD studies. The anatase was completely converted into rutile at 500°C. Annealing in oxygen to 600°C created a notable change in crystallinity of rutile with decreasing the reflections from titanium.

ACKNOWLEDGEMENT: This work was supported by the Korea Science and Engineering Foundation (KOSEF) grant funded by the Korea government (MOST) (No. R01-2007-000-20488-0).

LITERATURES CITED

- [1] S. Iijima, *Nature*, 354(1991), p 56.
- [2] M. Harada and M. Adachi, *Adv. Mater.* 12 (2000), p 839.
- [3] D. Gong, C.A. Grimes, O.K. Varghese, W. Hu, R.S. Singh, Z. Chen and E.C. Dickey, *J. Mater. Res.* 16 (2001), p 3331.

Synthesis of core-shell type ZnS-CdS photocatalyst with the stratified morphology

Tsugumi Hayashi¹, Yohei Baba¹, Toshiharu Taga¹,

Hideyuki Takahashi¹ and Kazuyuki Tohji¹

¹ 6-6-20 Aoba, Aramaki, Aoba-ku, Sendai 980-8579 Japan

Graduate School of Environmental Studies, Tohoku University

Recently, photocatalyst has vigorously investigated since it can be transformed the natural energy (solar energy) into clean energy (hydrogen energy). However, there are several problems for the effective hydrogen production by using photocatalyst. For example, ZnS can utilize only under UV-light irradiation, and co-catalyst such as Pt should be needed for CdS, nevertheless it has specific morphology (stratified structure) which showed the extremely higher catalytic activity than traditional type photocatalyst. To solve these disadvantages of CdS and ZnS, the creation of new band structure by using these materials, such as CdZnS type semiconductor, was tried to synthesized, and it was reported that CdZnS solid solution shows the high activity. However, CdZnS photocatalyst with stratified morphology was not synthesized until now. Objective of this study is to add stratified morphology to CdZnS type semiconductor for increase of activity.

Nature of precursor, such as morphology and phase, affect to that of stratified photocatalyst. Thus, precursor was designed and synthesized. FIGURE 1 shows the results of the calculation of metal complexes. Result of the calculation shows that formation of Zn oxide/hydroxide is faster than that of Cd, if the solution pH was changed from acid to basic and various type of oxide/hydroxide precursor can be synthesized by adjusting the rate of the pH increasing. Briefly, core(Zn)-shell(Cd) type oxide or hydroxide precursor will form when pH increasing rate become slow. Therefore, core(Zn)-shell(Cd) type precursor was tried to synthesize. FIGURE 2 shows the TEM image and EDX mapping of Zn and Cd of precursor particle synthesized at pH10.5. This result shows the position of Zn and Cd was almost same. Moreover, EDX mapping area of Cd was slightly larger than that of Zn. This result and result of ICP analysis, XRF analysis and XRD analysis show that core(microcrystal Zn)-shell(Cd(OH)₂) structure had successfully synthesized by obeying to the calculation.

FIGURE 3 shows TEM image of CdZnS particle synthesized from the precursor(pH10.5). The particles had capsule configuration. Thus, we succeeded at synthesis of CdZnS with stratified morphology.

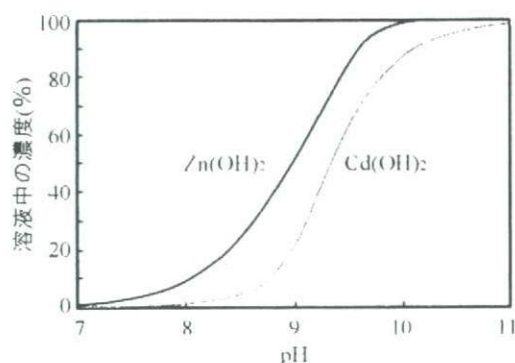


FIGURE 1 Result of the calculation of metal complex concentration

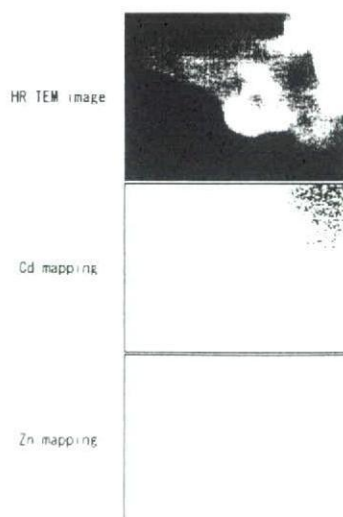


FIGURE 2 HR-TEM image and EDX mapping of Zn and Cd

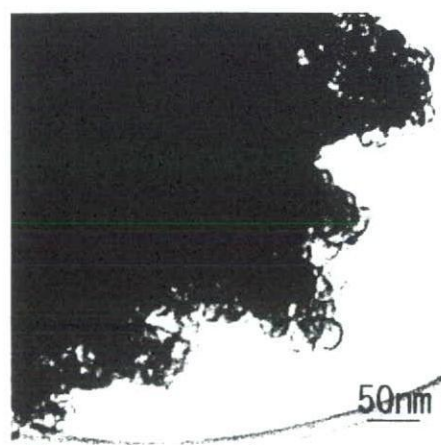


FIGURE 3 TEM image of CdZnS particles

Heat diffusion characteristics of magnetite nanoparticles in AC magnetic field

M. Suto¹, H. Kosukegawa¹, K. Maruta¹, M. Ohta¹,
K. Tohji¹ and B. Jeyadevan¹

¹Tohoku University, Sendai, Japan,

Magnetic fluid hyperthermia is a potential method to treat cancer, and demands detail studies on the development of efficient thermal seeds with heat dissipation and diffusion characteristics suitable for *in vivo* applications where cancer cells are killed selectively[1, 2]. Here, we report the results of numerical and experimental investigations on the heat diffusion characteristics of a heat source dispersing magnetite in hydro-gel and exposed to an AC magnetic field strength and frequency of 3.2 kA/m and 600 kHz respectively. The numerical estimation assuming one dimensional spherical model (Fig. 1) and constant heat evolution from the heat source suggested that a large temperature difference existed between the values at the center and the surface of the heat source. This reflected the local heating characteristics of magnetic fluid hyperthermia. On the other hand, similar behavior was also observed experimentally, except for a large temperature gradient at the magnetite-dispersed and magnetite-free hydro-gel interface for a rectangular model of PVA hydro-gel shown in Fig. 2.

Though a qualitative agreement between numerical estimation and experimental observation was recorded for magnetite concentrations 1, 2, and 4 wt. %, a quantitative difference existed in the temperature distribution (Fig. 3). The estimated value was always lower than the observed and the difference was greater for higher magnetite concentration. The ac magnetic measurements confirmed that the deviations between numerical and experimental values were mainly due to the difference in particle size distribution considered for numerical estimation rather than magnetic interaction. Thus, it was concluded that the algorithm used for the case which has no fluid flow is valid and studies are in progress to consider fluid flow conditions.

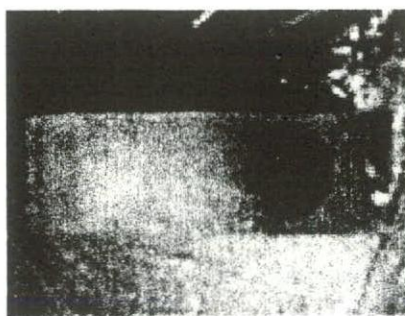


Fig. 2 Experimental specimen composed of spherical magnetite- dispersed hydro-gel.

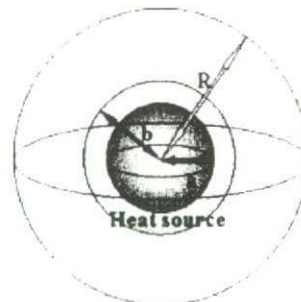


Fig. 1 Numerical model to investigate heat diffusion characteristics, a: domain of heat source MNPs are dispersed, b-a: domain of the magnetite free hydro-gel surrounding heat source, R-b: domain of air

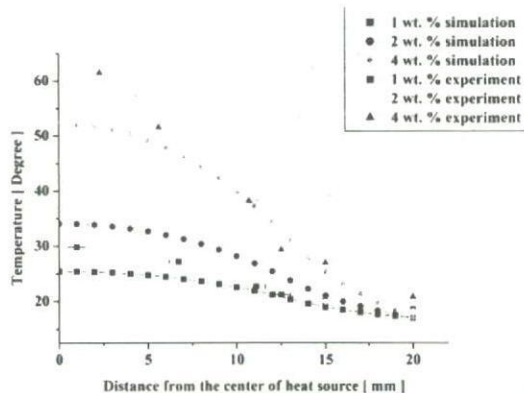


Fig.3 Temperature distribution along the radius of the heat source.

References

- [1] M. JOHANNSEN et al, Int. J. Hyperthermia, November 2005, 21(7): 637–647
- [2] K. Maier-Hauff et al, J Neurooncol 2007, 81:53–60

Multi-wall Carbon Nanotubes Monolith prepared by Spark Plasma Sintering (SPS) and its mechanical property

Motohiro Uo¹, Tsukasa Akasaka¹, Isao Tanaka², Fuminori Munekane³

Mamoru Omori⁴, Hisamichi Kimura⁴ and Fumio Watari¹

¹Graduate School of Dental Medicine, Hokkaido University, Sapporo, JAPAN

²Shimizu Cooperation, Tokyo, JAPAN

³Nano Carbon Technologies Co., Ltd, Tokyo, JAPAN

⁴Institute of Materials Research, Tohoku University, Sendai, JAPAN

Two types of multi-walled carbon nanotubes (MWCNTs) monolith without any binders was obtained by spark plasma sintering (SPS) treatment at 1100 to 2000°C under 40 to 80MPa of sintering pressure. Two MWCNTs in different diameter [20~30nm ϕ (CNT Co.ltd, Korea) or 100nm ϕ (Nano Carbon Technologies Co., Ltd, Japan)] were applied for SPS. SEM observation confirmed that this material maintained the nanosized tube microstructure of raw CNT powder after SPS treatment. The dense monolith was prepared with the mixture of thick (100nm ϕ) and thin (20~30nm ϕ). The mechanical properties of this material were estimated by dynamic hardness tester. The elastic modulus of the monolith from above CNTs mixture was significantly higher than the monolith prepared from thick CNTs. In our previous study, the mechanical properties of CNTs monolith was close to the natural human bone. Then, CNTs monolith could be a candidate bone substitute material and a bone tissue engineering scaffold material

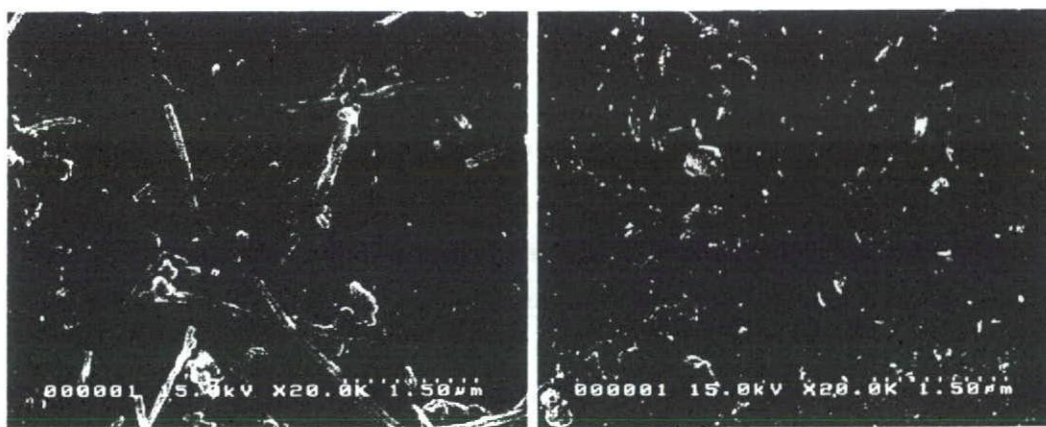


Fig.1 SEM images of SPS sintered MWCNTs (left:100% thick MWCNTs, right:mix. of 75% thick and 25% thin)

[1] W. Wang, F. Watari, M. Omori, S. Liao, Y. Zhu, A. Yokoyama, M. Uo, H. Kimura, A. Ohkubo: Journal of Biomedical Materials Research Part B, 82B (2007), p.223

**Fabrication and mechanical and biological properties of
porous chitosan/ HAp nanocomposites**

Haruhiko Kashiwazaki¹, Yusuke Kishiya¹, Keisuke Yamaguchi¹,
Tadashi Iizuka², Junzo Tanaka³, Nobuo Inoue¹

¹ Department of Oral Health Science, Graduate School of Dental Medicine, Hokkaido University, N13 W7, Kita-ku, Sapporo, 060-8586, Japan

² Support Section for Education and Research, Graduate School of Dental Medicine, Hokkaido University, N13 W7, Kita-ku, Sapporo, 060-8586, Japan

³ Department of Inorganic Materials, Tokyo Institute of Technology, 2-12-1, Ookayama, Meguro-ku, Tokyo 152-8550, Japan

Introduction

Previously, we developed a homogeneous chitosan/HAp composite using a co-precipitation method[1]. In recent years, particular attention was paid to the synthesis of biomaterials with porous morphology to allow the ingrowth of bone tissue which further improves the mechanical fixation of the implant at the implantation site. The aim of the present study is to prepare homogeneous HAp/chitosan composites with porous structure.

Materials and methods

To introduce porosity into the chitosan/HAp composite described above, co-precipitation and porogen leaching method were used. The microstructure and mechanical properties were characterized by using scanning electron microscopy (SEM) and a three-point bending strength test. *In vivo* biocompatibility of the composites was also investigated.

Results

According to SEM observations, the porous chitosan/HAp nanocomposites with 60.6% and 87.1% porosity showed the interconnective pores with pore diameters in the range of 100-200 μm . The composites were found to be mechanically flexible and easily could be formed into any desired shape. The mechanical strength could be enhanced by heat treatment in a saturated steam. Tissue responses to the nanocomposites subcutaneously implanted in the backs of SD rats were examined. Little inflammatory cell infiltration was observed around the nanocomposites subcutaneously implanted in the backs of SD rats.

Conclusion

Novel chitosan/HAp nanocomposites with various porosity were fabricated, which were found to be mechanically flexible, biocompatible and biodegradable.

[1] Yamaguchi, I. et al. Preparation and microstructure analysis of chitosan/hydroxyapatite nanocomposites. *J Biomed Mater Res* 2001;55:20-27.

Chemical Modification of Carbon Nanotubes and Their Use in Adhesive Interaction Force Measurements Using an Atomic Force Microscope

Hiroaki Azehara¹, Koichiro Ide² and Hiroshi Tokumoto¹

¹ Nanotechnology Research Center, Research Institute for Electronic Science (RIES),

Hokkaido University, Kita 21 Nishi 10, Kita-ku, Sapporo 001-0021, Japan

²Graduate School of Information Science and Technology (IST),

Hokkaido University, Kita 14 Nishi 9, Kita-ku, Sapporo 060-0814, Japan

Toxicity of carbon nanomaterials has been a great concern because they have potential for biomedical applications. In fact, the size of the carbon materials is an important factor in their toxicity. Also, the adhesive interaction of the carbon materials should be an important physical property because they tend to form aggregates and therefore the size of them may be controlled by the interaction force. Especially, it is known that strong hydrophobic interaction of carbon materials is observed under aqueous environment. The hydrophobic interaction can be attenuated by surface treatment such as oxidation treatment and modification by chemical reagents. Meanwhile, we have developed an analytical mean to measure the adhesive interaction between the tip of a carbon nanotube (CNT tip) and other material surfaces using an atomic force microscope (AFM).

To investigate adhesive interaction between surfaces, chemically modified AFM probe tips have long been utilized [1]. In many cases, gold-coated AFM probes that are chemisorbed by thiol compounds are employed for chemical force microscopy or molecular recognition imaging. On the other hand, we have recently demonstrated that the CNT tip that we prepared in our laboratory can be used as a chemically modified AFM probe even in a contact mode operation [2]. Then, it was also concluded that the CNT tip retained carboxyl group at the tip end through force titration measurements in buffer solutions and further chemical derivatization was preliminarily demonstrated. Using this kind of CNT tip, we have been investigating a facile method for converting the tip-end functional groups. In this symposium, we will report the procedures of CNT tip fabrication, their chemical modification, and the measured adhesive force between carboxyl groups using these CNT tips with a quantitative analysis.

Literature References

- [1] H. Takano, J. R. Kenseth, S.-S. Wong, J. C. O'Brien and M. D. Porter: Chem. Rev. Vol. 99 (1999), p. 2845
- [2] H. Azehara, Y. Kasanuma, K. Ide, K. Hidaka and H. Tokumoto: Jpn. J. Appl. Phys., in press.

Ryuichi Fujisawa, Morimichi Mizuno, Masato Tamura

Department of Oral Biochemistry and Molecular Biology, School of Dentistry, Hokkaido University, N13W7, Sapporo, Japan, E-mail: rfuji@den.hokudai.ac.jp

Introduction: Matrices of bone and tooth contain various acidic proteins that can induce and control nucleation of hydroxyapatite crystals, the major mineral component of these tissues. For example, dentin phosphoprotein, the major acidic protein of dentin, is a potent inducer of the crystal nucleation, when it is attached to solid surfaces. These proteins contain many acidic groups. These groups are responsible to binding of calcium ions and attachment of the proteins to the crystals. In the present study we attempted to use an anionic dendrimer as a model for these proteins to investigate the role of acidic groups in mineralization.

Methods: Dentin phosphoprotein was extracted and purified from bovine dentin. PAMAM dendrimer 4.5 generation was used as a model dendrimer. This dendrimer has 128 carboxyl groups on the molecular surface. *In vitro* mineralization was performed by using a system composed of agar gels in wells of a 96-well plate. The dendrimer or the acidic proteins were included in the gels. Calcium and phosphate ions were diffused in the gels. Another system is composed of a nylon membrane spotted with the dendrimer or the acidic proteins. The membrane was sandwiched with filter papers containing calcium or phosphate ions. The calcium phosphate precipitated on the membrane was stained with Alizarin red.

Results: In the gel system, the dendrimer enhanced the calcium phosphate deposition at low calcium concentration. However, it reduced the deposition at high calcium concentration. This effect was similar to that of dentin phosphoprotein. In the membrane system, the dendrimer enhanced the deposition. Dentin phosphoprotein, egg phosphovitin and poly glutamic acid also enhanced the deposition. Their effect was much higher than that of the dendrimer. At high concentration, dentin phosphoprotein had inhibitory effect on the deposition. Poly aspartic acid had inhibitory effect. Protamine, a peptide rich in arginine, reduced the effects of these acidic proteins.

Discussion: The dendrimer can mimic the effect of the acidic proteins, at least partially. Clusters of acidic amino acids are present in acidic matrix proteins of bone and tooth. These clusters bind many calcium ions and may function as sites of nucleation of calcium phosphate crystals. Clusters of carboxyl groups on the surface of the dendrimer may have similar function. However, the effect was weak in comparison with that of the dentin phosphoprotein. Presence of the carboxyl groups is not enough for the full function. Three-dimensional arrangement of the acidic groups may be important for the function. In contrast to the dendrimer, acidic groups of the acidic proteins can adopt a flexible arrangement. They may form a conformation that favors the nucleation of the crystals.

VOC removal activity of fired scallop shell: assignment of effective component

Tomoya Takada, Atsushi Furusaki, Yasuaki Tanaka

Department of Materials Chemistry, Asahikawa National College of Technology,

2-2-1-6, Syunkodai , Asahikawa 071-8142, Japan

Introduction. Scallop shell powder fired at relatively high temperatures (so-called scallop shell ceramics) has been known to show several desirable characteristics: volatile organic compounds (VOC) removal activity, antibacterial and antifungal activity, deodorizing activity, and so on. For example, fired scallop shell removes formaldehyde (HCHO), toluene (C₆H₅CH₃), ethylbenzene (C₆H₅C₂H₅) and other gaseous organic compounds from air. However, the effective components are not definitively assigned, and detailed mechanism of the VOC removal is still unclear. In this study, the VOC (HCHO) removal activity of scallop shell fired at several temperatures has been compared. The possible effective component in fired scallop shell has been assigned on the basis of experimental results.

Experimental. Scallop shell powder was made by ball milling of raw shell. The powder was then filtered to obtain the powder with the particle size smaller than 0.7 mm and fired at several temperatures between 200 and 1000 °C for 2 hours. The removal of HCHO from air by the powders was measured in a Tedlar bag. The each powder (2.0 g) was put in a 10 dm³ Tedlar bag and then gaseous HCHO was introduced in the bag to make the HCHO concentration approximately 1 ppm. The time-course of the HCHO concentration was monitored with a passive dosimeter. X-ray diffraction (XRD) patterns of the powders were measured with an X-ray diffractometer (RIGAKU RAD-B).

Results and discussion. Here, the results obtained using raw and fired (300, 600 and 900 °C) scallop shell powders are shown as examples. When the raw powder was used, the HCHO concentration gradually changed from 1.2 ppm to 0.5 ppm within 120 min. The similar tendency was observed in the cases of the powders immediately after firing at 300 and 900 °C: 1.4 ppm → 0.4 ppm (300°C) and 1.1 ppm → 0.3 ppm (900 °C). The powder fired at 600 °C did not show the HCHO removal activity. When the powders stored for 3 months in air after firing were used, the HCHO removal activity was changed from that of the powders immediately after firing in certain cases. The HCHO removal activity of the powders fired at 300 and 600 °C was similar to the cases of the powders immediately after firing; 1.0 ppm → 0.4 ppm (300 °C) and 1.3 ppm → 1.1 ppm (600 °C) within 120 min. On the other hand, the HCHO removal activity of the powder fired at 900 °C was clearly changed after storing for 3 months. The HCHO concentration rapidly reached zero within 20 min. From the XRD measurements, it was found that the main component of the powders fired at 300 and 600 °C was CaCO₃, while the main component of the powder fired at 900 °C was CaO. CaCO₃ did not change to any other compounds even after 3 months. CaO changed to Ca(OH)₂ after 3 months by the reaction $\text{CaO} + \text{H}_2\text{O} \rightarrow \text{Ca(OH)}_2$. Ca(OH)₂ seems to be the effective component for the HCHO removal.